Mathematics in Applied Sciences and Engineering
Online First, pp.**1-23**

https://ojs.lib.uwo.ca/mase
https://doi.org/10.5206/mase/22989

A STUDY ON STATISTICAL PROPERTIES OF A NEW CLASS OF q-FRÉCHET DISTRIBUTION

HENNIA DOUINI AND IBRAHIM SADOK

Abstract. This paper introduces the q-Fréchet distribution, a two-parameter generalization of the classical Fréchet model that incorporates a pathway parameter q within the framework of Tsallis statistics. The proposed distribution offers enhanced flexibility for modeling real-world data with non-standard tail behavior, accommodating both sub-exponential ($q < 1$) and super-exponential ($1 < q < 2$) regimes. We derive its fundamental statistical properties, including survival, hazard, quantile, and moment functions, and investigate its extreme value behavior. Parameter estimation is addressed through multiple methods, with a focus on maximum likelihood and Bayesian inference, supported by a comprehensive simulation study. Applied to reliability datasets (carbon fiber strength and airborne transceiver repair times) the q-Fréchet demonstrates a consistently superior fit compared to the classical Fréchet distribution, confirming its practical utility in modeling complex, heavy-tailed data. This work establishes the q-Fréchet as a robust and adaptable model for applications in reliability engineering, survival analysis, and beyond.

1. Introduction

The statistical modeling of extreme events finds one of its most pivotal tools in the Fréchet distribution. Originating from the pioneering work of Maurice René Fréchet in the 1920s, its mathematical formalization was cemented by Fisher and Tippett's landmark paper on limiting distributions of maxima [8]. It represents the Type II case of the Generalized Extreme Value (GEV) distribution, a unification rigorously established later by Gnedenko [9]. Characterized by a heavy right tail, the Fréchet distribution is the natural limiting model for the maximum of independent, identically distributed random variables whose tails decay polynomially, such as those following Pareto, Cauchy, or Student's t distributions. This property has driven its adoption across a breathtaking array of disciplines: from hydrology and meteorology for modeling maximum river flows, rainfall, and wind speeds [14, 10], to reliability engineering for predicting the strength of materials and system failure times [19], and finance for assessing market risk and catastrophic insurance losses [6].

The enduring relevance of the Fréchet model has inspired a vast ecosystem of extensions and generalizations, each designed to inject greater flexibility for capturing complex data features like bimodality, bounded support, or varying hazard rates. Early multiplicative transformations led to the exponentiated Fréchet distribution, which introduces an additional shape parameter for more versatile hazard function modeling [16]. The transmuted Fréchet distribution employs a quadratic rank transmutation map to generate more flexible families capable of modeling data with lighter or heavier tails and potential bimodality [15]. For scenarios with known physical limits or censored data, truncated variants like the left-truncated [11] and right-truncated Fréchet-Weibull [31] distributions have been developed. More recently, generator methods using other dominant statistical families have produced generalizations such

Received by the editors 12 May 2025; accepted 8 December 2025; published online 10 December 2025.
2020 *Mathematics Subject Classification.* 62E10, 62F10, 62N05, 62P30.
Key words and phrases. q-Fréchet distribution, statistical properties, parameter estimation, modelling data.

as the beta-Fréchet and Kumaraswamy-Fréchet distributions, which offer even richer shapes by adding two or more parameters [see analogous methods in [24]]. Despite their utility, these extensions largely remain within the confines of classical, extensive statistical mechanics, relying on the exponential and logarithmic functions as their core building blocks. These modifications typically introduce additional shape or location parameters, improving fit but often within the framework of classical exponential family statistics. The probability density function (pdf) and cumulative distribution function (cdf) of the Fréchet distribution are given respectively, by

$$f(x;\lambda,\alpha) = \lambda\alpha x^{-(\alpha+1)} e^{-\lambda x^{-\alpha}}; \quad \lambda,\alpha>0,\ x>0 \tag{1.1}$$

$$F(x;\lambda,\alpha) = e^{-\lambda x^{-\alpha}}. \tag{1.2}$$

A profound paradigm shift occurred with the advent of non-extensive statistical mechanics, introduced by Constantino Tsallis in 1988 [33, 32]. This framework generalizes the Boltzmann-Gibbs entropy for systems with long-range interactions, memory effects, or fractal geometries—common features in complex systems across physics, biology, and economics. The cornerstone of this theory is the q-exponential function, defined as

$$\exp_q(x) = \begin{cases} [1+(1-q)x]^{\frac{1}{1-q}}, & 1+(1-q)x>0 \\ 0 & \text{otherwise,} \end{cases} \tag{1.3}$$

and its inverse, the q-logarithm. The entropic index or pathway parameter q provides a continuous deformation: as $q \to 1$, classical exponential statistics are recovered, while deviations ($q \neq 1$) capture sub-exponential ($q<1$) or super-exponential ($q>1$) behaviors, often manifesting as power-law tails. This mathematical structure, explored in depth by Borges [4], offers a parsimonious yet powerful mechanism for modeling data that eludes traditional exponential-family distributions.

The q-exponential has spawned an entire field of q-generalized probability distributions, revolutionizing data analysis in areas where classical models fail. The q-exponential distribution itself became a foundational model for non-Markovian processes and systems in non-equilibrium stationary states [3]. In physics and finance, the q-Gaussian distribution has become indispensable for modeling systems with fat-tailed return distributions and anomalous diffusion [28]. For reliability and survival analysis, the q-Weibull distribution has demonstrated exceptional flexibility in modeling bathtub, increasing, and decreasing hazard rates, finding applications from engineering to medicine [13, 18, 30]. Subsequent work has generalized other key models, including the q-Gamma [2], Generalized q-logistic [17], and q-Rayleigh [25] distributions.

Most pertinent to this work is the generalization of extreme value theory within this framework. Provost et al. [19] introduced the q-generalized extreme value distribution (q-GEVD), embedding the entire GEV family within Tsallis statistics. While a monumental theoretical contribution, a dedicated, in-depth exploration of its Fréchet sub-case (the q-Fréchet distribution) is absent from the literature. The distinct properties, parameter estimation challenges, and specific application niches of the Fréchet model warrant focused investigation. Furthermore, methodological studies on q-distributions have predominantly relied on Maximum Likelihood Estimation (MLE). A comprehensive evaluation of alternative estimators (crucial for robustness, small-sample performance, and practical application) is lacking. This includes Bayesian methods, which incorporate prior knowledge and provide natural uncertainty quantification via MCMC techniques; the Method of Moments (MoM); and percentile-based minimum distance estimators, known for their robustness to model misspecification.

This manuscript addresses these identified gaps through three principal contributions. First, it provides the formal theoretical introduction and characterization of the two-parameter q-Fréchet distribution, a new member of the q-generated family. We offer a complete derivation of its foundational

properties—including its probability density, cumulative distribution, survival, hazard, and quantile functions for both the sub-exponential ($q < 1$) and super-exponential ($1 < q < 2$) regimes—and establish its moments, limiting behavior, and closure under minima and maxima operations. Second, it establishes a comprehensive methodological framework by implementing and rigorously comparing a suite of estimation techniques: MLE, Bayesian inference (with weakly informative priors and Metropolis-Hastings MCMC), the MoM, and Percentile-Based Least Squares (P-LS). An extensive simulation study evaluates their finite-sample performance across key metrics (bias, RMSE, coverage probability). Third, it delivers an empirical validation demonstrating the q-Fréchet's practical utility and superior fit over the classical Fréchet model using two real-world reliability datasets concerning carbon fiber strength and airborne communication transceiver repair times, leveraging all four estimation methods and standard goodness-of-fit criteria.

The remainder of this paper is structured as follows. Section 2 formally introduces the q-Fréchet distribution, detailing its probability density function, cumulative distribution function, and key derived functions such as the survival and hazard rate functions for both parameter regimes. Section 3 delves into the mathematical and statistical properties of the distribution, including its limiting behavior, quantile function, moments, and extreme value properties. Section 4 is dedicated to parameter estimation, presenting the methods of Maximum Likelihood Estimation, Bayesian inference, Method of Moments, and Percentile-Based Least Squares. Section 5 details an extensive simulation study designed to evaluate and compare the finite-sample performance of these estimation techniques. Section 6 demonstrates the practical application of the q-Fréchet distribution by modeling two real-world datasets from reliability engineering and comparing its goodness-of-fit to the classical Fréchet model. Finally, Section 7 concludes the paper by summarizing the key findings and discussing potential avenues for future research.

2. The q-Fréchet distribution

2.1. **Distributional characteristics.** The pdf of the q-Fréchet distribution is defined as

$$f_q(x) = (2-q)\lambda\alpha x^{-(\alpha+1)} \exp_q\left[-\lambda x^{-\alpha}\right],\ x > 0 \tag{2.1}$$

where $\lambda > 0$ and $q < 2$ are shape parameters, and $\alpha > 0$ is a scale parameter.

Using $\exp_q(.)$ function in equation (1.3), the pdf of the q-Fréchet distribution, for $x > 0$ and for $q < 1$, can be rewritten as

$$f_q(x) = (2-q)\lambda\alpha x^{-(\alpha+1)} \left[1-(1-q)\lambda x^{-\alpha}\right]^{\frac{1}{1-q}},\ q < 1 \text{ and } x \in \left[0, (\lambda(1-q))^{\frac{1}{\alpha}}\right] \tag{2.2}$$

For $x > 0$ and $1 < q < 2$, the pdf of the q-Fréchet distribution is expressed as:

$$f_q(x) = (2-q)\lambda\alpha x^{-(\alpha+1)} \left[1+(q-1)\lambda x^{-\alpha}\right]^{-\frac{1}{q-1}},\ 1 < q < 2 \text{ and } x \in [0, +\infty) \tag{2.3}$$

The cumulative distribution function (cdf) of the q-Fréchet distribution, when $q < 1$ is defined as

$$F_q(x) = \left[1-(1-q)\lambda x^{-\alpha}\right]^{\frac{2-q}{1-q}} \tag{2.4}$$

If $1 < q < 2$, the cdf function of the q-Fréchet distribution, formulated as follows:

$$F_q(x) = \left[1+(q-1)\lambda x^{-\alpha}\right]^{\frac{q-2}{q-1}} \tag{2.5}$$

2.2. **Survival function.** In the context of the q-Fréchet distribution, the survival function (sf), denoted by $S(x)$, represents the probability that an individual or entity survives beyond time t. Its mathematical expression is as follows

$$S(x) = P(X > t) = 1 - F(x)$$

$$S_q(x) = 1 - \left[1 - (1-q)\lambda x^{-\alpha}\right]^{\frac{2-q}{1-q}}, \quad \text{for } q < 1,$$
$$S_q(x) = 1 - \left[1 + (q-1)\lambda x^{-\alpha}\right]^{\frac{2-q}{1-q}}, \quad \text{for } 1 < q < 2$$

2.3. **Hazard function.** The concept of risk within the context of survival analysis is characterized by the hazard rate function (hrf), $h(x)$. This function measures the immediate risk of an event (e.g., death) for an individual who has survived until that time. Its formal representation is as follows

$$h(x) = P(X > t) = \frac{f(x)}{S(x)}$$

The hrf of q-Fréchet distribution for $q < 1$ is defined as

$$h_q(x) = \frac{(2-q)\lambda\alpha x^{-(\alpha+1)}\left[1 - (1-q)\lambda x^{-\alpha}\right]^{\frac{1}{1-q}}}{1 - \left[1 - (1-q)\lambda x^{-\alpha}\right]^{\frac{2-q}{1-q}}}$$

In the case of $1 < q < 2$, the hrf of q-Fréchet distribution is characterized by

$$h_q(x) = \frac{(2-q)\lambda\alpha x^{-(\alpha+1)}\left[1 - (q-1)\lambda x^{-\alpha}\right]^{-\frac{1}{q-1}}}{1 - \left[1 + (q-1)\lambda x^{-\alpha}\right]^{\frac{2-q}{1-q}}}$$

2.4. **Cumulative hazard function.** The probability of an event occurring before a given time is quantified by the cumulative hazard function (chf), presented below

$$H(x) = -\ln(1 - F(x))$$

The chf for the q-Fréchet distribution, with $q < 1$, is expressed as follows

$$H_q(x) = \ln\left[1 - \left[1 - (1-q)\lambda x^{-\alpha}\right]^{\frac{2-q}{1-q}}\right].$$

For the case where $1 < q < 2$, the chf of the q-Fréchet distribution is given by

$$H_q(x) = \ln\left[1 - \left[1 + (q-1)\lambda x^{-\alpha}\right]^{\frac{2-q}{1-q}}\right]$$

2.5. **Graphical Study of q-Fréchet distribution under various functions.** Driven by a desire to understand the nuanced behaviour of the q-Fréchet distribution, we embark on a detailed exploration of its key functions (pdf, cdf, sf, and hrf) across a range of parameter values. By meticulously analysing the illustrative figures presented below, we uncover fascinating insights into how varying parameters sculpt the behaviour of this versatile distribution. Complementing our theoretical exploration, we presented illustrative figures to visually depict the distribution's characteristics, enhancing accessibility and understanding.

Figures 1 and 2 showcase the graphical representation of the key functions of the q-Fréchet distribution for cases where $q < 1$ and $1 < q < 2$, respectively. Examining the probability density function graphs (1 (A), 1 (B), 2 (A),and 2 (B)), it becomes evident that the distribution exhibits skewness and a high degree of adaptability to diverse parameter values.

In Figures 1 (C), 1 (D), 2 (C) and 2 (D), we observe cumulative density plots that serve to validate the distribution's suitability as a probability distribution. Additionally, Figures 1 (E) and 2 (E) portray the survival function, revealing distinct patterns of fast and slow decreases. The hazard rate function graphs (1 (F), 2 (F)) further contribute to the distribution's versatility, showcasing a range of shapes including increasing, decreasing, and constant. This variability allows for the effective fitting of datasets with diverse forms, a characteristic that the q-Fréchet distribution adeptly demonstrates. In essence, our exploration underscores the distribution's capability to accommodate different data sets, making it a valuable tool in statistical analysis.

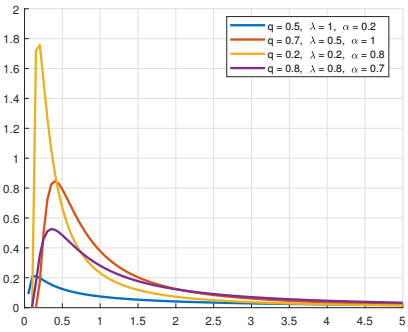

(A) Graph of the pdf of the q-Fréchet distribution when all the parameters are changed

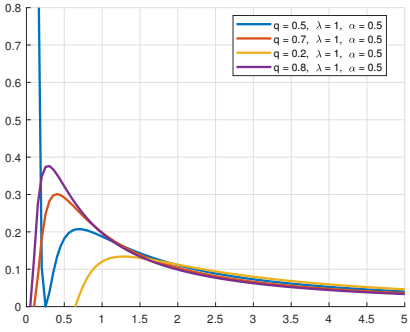

(B) Graph of the pdf of the q-Fréchet distribution when changing the q values and λ, α are fixed

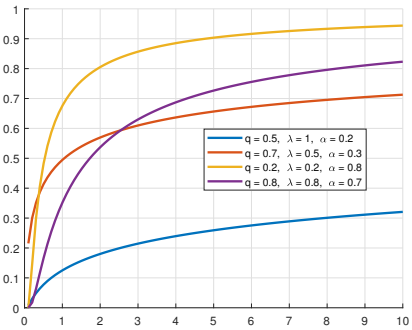

(C) Graph of the cdf of the q-Fréchet distribution when all the parameters are changed

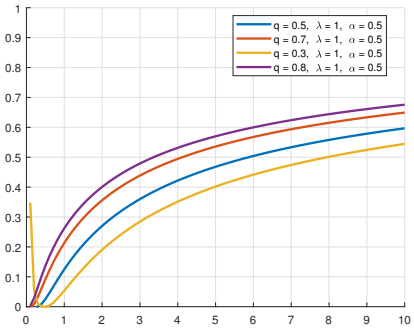

(D) Graph of the cdf of the q-Fréchet distribution when changing the q values and λ, α are fixed

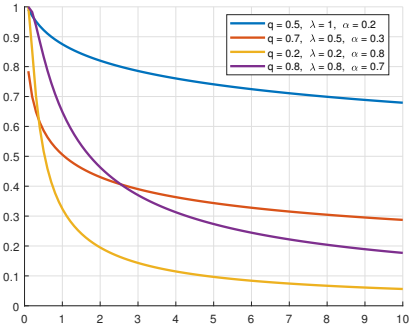

(E) Graph of the sf of the q-Fréchet distribution with different parameter values

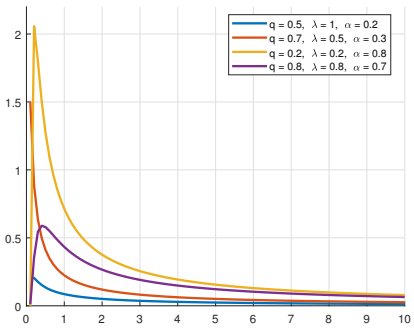

(F) Graph of the hrf of the q-Fréchet distribution with different parameter values

FIGURE 1. Graphical representation of the key functions of the q-Fréchet distribution: $q < 1$

3. PROPERTIES

This section delves into the mathematical and statistical characteristics of the q-Fréchet distribution.

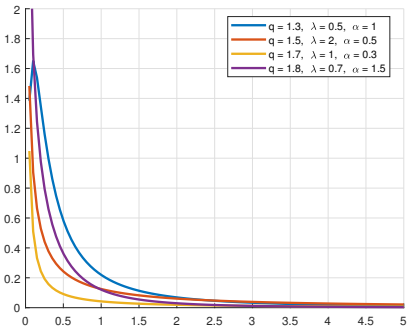

(A) Graph of the pdf of the q-Fréchet distribution when all the parameters are changed

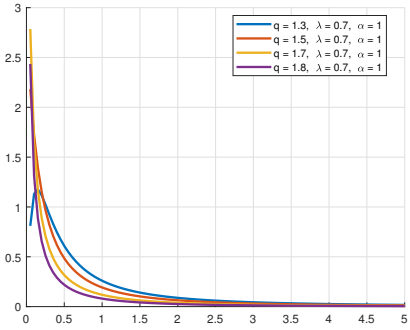

(B) Graph of the pdf of the q-Fréchet distribution when changing the q values and λ, α are fixed

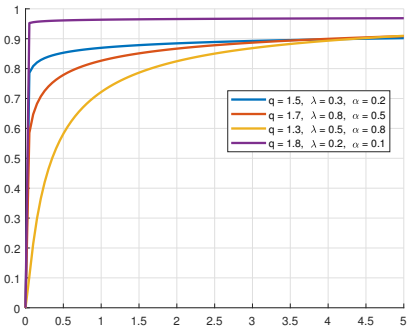

(C) Graph of the cdf of the q-Fréchet distribution when all the parameters are changed

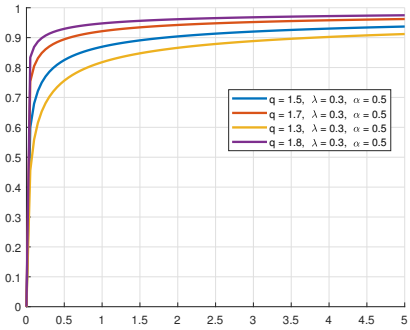

(D) Graph of the cdf of the q-Fréchet distribution when changing the q values and λ, α are fixed

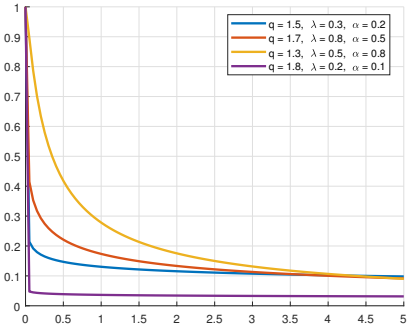

(E) Graph of the sf of the q-Fréchet distribution with different parameter values

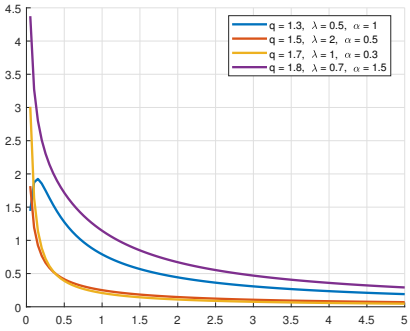

(F) Graph of the hrf of the q-Fréchet distribution with different parameter values

FIGURE 2. Graphical representation of the key functions of the q-Fréchet distribution: $1 < q < 2$

3.1. **Limiting Behaviour.**

Lemma 3.1. *As the parameter q approaches 1, the pdf of the q-Fréchet distribution, (denoted as $f_q(x)$), converges to the standard Fréchet distribution.*

Proof. For $q < 1$, the limiting pdf for $q = 1$ is

$$\begin{aligned}\lim_{q\to 1} f_q(x) =& \lambda\alpha x^{-(\alpha+1)} \lim_{q\to 1} \left\{ \left[1-(1-q)\lambda x^{-\alpha}\right]^{\frac{-1}{(1-q)\lambda x^{-\alpha}}} \right\}^{-\lambda x^{-\alpha}} \\ =& \lambda\alpha x^{-(\alpha+1)} \exp\left(-\lambda x^{-\alpha}\right)\end{aligned}$$

a Fréchet pdf.

The established proof methodology can be directly applied to the range $1 < q < 2$, yielding an analogous conclusion. □

3.2. **Quantile Function.** The quantile function of X, denoted as $Q(u)$ and defined as $Q(u) = F^{-1}(u)$, can be derived by inversely solving equations (2.4) and (2.5) as follows

$$Q_q(u) = \left[\frac{1-u^{\frac{1-q}{2-q}}}{(1-q)\lambda}\right]^{1/\alpha}, \quad \text{for } q < 1, \tag{3.1}$$

$$Q_q(u) = \left[\frac{u^{\frac{1-q}{2-q}}-1}{(q-1)\lambda}\right]^{1/\alpha}, \quad \text{for } 1 < q < 2 \tag{3.2}$$

3.3. **Moments.** This section presents the moment function for the q-Fréchet distribution, where moments serve as quantitative indicators associated with the function's shape. The moments of the q-Fréchet distribution can be derived as follows:

$$E(X^s) = \int_0^{+\infty} x^s f_q(x)dx$$

If $q < 1$,

$$\begin{aligned}E(X^s) =& \int_0^{(\lambda(1-q))^{\frac{1}{\alpha}}} x^s(2-q)\lambda\alpha x^{-(\alpha+1)}\left[1-(1-q)\lambda x^{-\alpha}\right]^{\frac{1}{1-q}} dx \\ =& \frac{q-2}{(1-q)^{1+s\alpha}\lambda^{s\alpha}} B\left(s\alpha+1, \frac{2-q}{1-q}\right)\end{aligned}$$

where,

$$B(p,q) = \int_0^1 t^{p-1}(1-t)^{q-1}\,dt = \int_0^{+\infty} \frac{t^{q-1}}{(1+t)^{p+q}}\,dt$$

denotes the beta function. It follows that the mean and variance of the q-Fréchet random variable when $q < 1$ are

$$\begin{aligned}E(X) =& \frac{q-2}{(1-q)^{1+\alpha}\lambda^{\alpha}} B\left(\alpha+1, \frac{2-q}{1-q}\right) \\ Var(X) =& \frac{q-2}{(1-q)^{1+2\alpha}\lambda^{2\alpha}} \left[B\left(2\alpha+1, \frac{2-q}{1-q}\right) - \frac{q-2}{1-q} B^2\left(\alpha+1, \frac{2-q}{1-q}\right)\right]\end{aligned}$$

If $1 < q < 2$,

$$\begin{aligned}E(X^s) =& \int_0^{+\infty} x^s(2-q)\lambda\alpha x^{-(\alpha+1)}\left[1+(q-1)\lambda x^{-\alpha}\right]^{-\frac{1}{q-1}} dx \\ =& \frac{2-q}{(q-1)^{1+s\alpha}\lambda^{s\alpha}} B\left(\frac{1}{q-1} - s\alpha - 1, s\alpha+1\right)\end{aligned}$$

provided $1/(q-1) - s\alpha > 1$. Consequently, the mean and variance of the q-Fréchet random variable can be expressed as follows

$$E(X) = \frac{2-q}{(q-1)^{1+\alpha}\lambda^{\alpha}} B\left(\frac{1}{q-1} - \alpha - 1, \alpha + 1\right)$$
$$Var(X) = \frac{(2-q)}{(q-1)^{1+2\alpha}\lambda^{2\alpha}} \left[B\left(\frac{1}{q-1} - 2\alpha - 1, 2\alpha + 1\right) - \frac{2-q}{q-1} B^2\left(\frac{1}{q-1} - \alpha - 1, \alpha + 1\right)\right]$$

3.4. **Extreme value properties.**

Theorem 3.2. *Let $\{X_i,\, i = 1, ..., n\}$ be independent and identically distributed random variables (r.v.) following the q-Fréchet distribution, then $U = \min_{1 \leqslant i \leqslant n} X_i$ has also the same distributional form.*

Proof. For $q < 1$ the survival function is

$$S_q(x) = 1 - \left[1 - (1-q)\lambda x^{-\alpha}\right]^{\frac{2-q}{1-q}}.$$

Then,

$$\begin{aligned} S_q(x) &= P\left[\min_{1 \leqslant i \leqslant n} X_i > x\right] \\ &= \prod_{i=1}^{n} P\left[X_i > x\right] \\ &= \prod_{i=1}^{n} 1 - \left[1 - (1-q)\lambda x^{-\alpha}\right]^{\frac{2-q}{1-q}} \\ &= 1 - \left[1 - (1-q)\lambda x^{-\alpha}\right]^{n\frac{2-q}{1-q}} \longrightarrow e^{-n\lambda x^{-\alpha}} \text{ as } q \longrightarrow 1 \end{aligned}$$

For $1 < q < 2$ the survival function is $S_q(x) = 1 - \left[1 + (q-1)\lambda x^{-\alpha}\right]^{\frac{2-q}{1-q}}$. Then,

$$S_q(x) = 1 - \left[1 + (q-1)\lambda x^{-\alpha}\right]^{n\frac{2-q}{1-q}} \longrightarrow e^{-n\lambda x^{-\alpha}} \text{ as } q \longrightarrow 1$$

□

Theorem 3.3. *Let $\{X_i,\, i = 1, ..., n\}$ be independent and identically distributed random variables (r.v.) following the q-Fréchet distribution, then $V = \max_{1 \leqslant i \leqslant n} X_i$ has also the same distributional form.*

Proof. For $q < 1$ the cdf is

$$F_q(x) = \left[1 - (1-q)\lambda x^{-\alpha}\right]^{\frac{2-q}{1-q}}.$$

Then,

$$\begin{aligned} F_q(x) &= P\left[\max_{1 \leqslant i \leqslant n} X_i \leqslant x\right] \\ &= \prod_{i=1}^{n} P\left[X_i \leqslant x\right] \\ &= \prod_{i=1}^{n} \left[1 - (1-q)\lambda x^{-\alpha}\right]^{\frac{2-q}{1-q}} \\ &= \left[\left[1 - (1-q)\lambda x^{-\alpha}\right]^{\frac{2-q}{1-q}}\right]^{n} \longrightarrow \left[e^{-\lambda x^{-\alpha}}\right]^{n} \text{ as } q \longrightarrow 1 \end{aligned}$$

Similarly for $1 < q < 2$ the cdf of V is

$$F_q(x) = \left[\left[1 + (q-1)\lambda x^{-\alpha}\right]^{\frac{q-2}{q-1}}\right]^n \longrightarrow \left[e^{-\lambda x^{-\alpha}}\right]^n \text{ as } q \longrightarrow 1$$

□

4. Estimation of Parameters

4.1. **Maximum Likelihood Estimation.** This section explores the estimation of the unknown parameters in the q-Fréchet distribution through the application of the maximum likelihood estimation method (MLE) [26, 23].

Let $x_1, x_2, \ldots, x_n$ represent a random sample obtained from the q-Fréchet distribution. The subsequent expression outlines the logarithm of the likelihood function corresponding to the pdf represented in equation (2.2) for $q < 1$ is

$$\ln L = n\ln(2-q) + n\ln\lambda + n\ln\alpha - (\alpha+1)\sum_{i=1}^{n}\ln(x_i) + \frac{1}{1-q}\sum_{i=1}^{n}\ln\left(1-(1-q)\lambda x_i^{-\alpha}\right) \tag{4.1}$$

The maximum likelihood estimates of the parameters (q, λ, α) are found by taking a partial derivative of $\ln L$ with respect to q, λ and α, equating the derivatives to zero, and evaluating them at $\widehat{q}$, $\widehat{\lambda}$ and $\widehat{\alpha}$

$$\begin{aligned}
\frac{\partial \ln L}{\partial q} =& -\frac{n}{2-q} + \frac{1}{(1-q)^2}\sum_{i=1}^{n}\left[\ln\left(1-(1-q)\lambda x_i^{-\alpha}\right)\right] + \frac{1}{1-q}\sum_{i=1}^{n}\frac{\lambda x_i^{-\alpha}}{1-(1-q)\lambda x_i^{-\alpha}}\\
\frac{\partial \ln L}{\partial \lambda} =& \frac{n}{\lambda} - \sum_{i=1}^{n}\frac{x_i^{-\alpha}}{1-(1-q)\lambda x_i^{-\alpha}}\\
\frac{\partial \ln L}{\partial \alpha} =& \frac{n}{\alpha} - \sum_{i=1}^{n}\ln x_i + \lambda\sum_{i=1}^{n}\left[\frac{x_i^{-\alpha}\ln x_i}{1-(1-q)\lambda x_i^{-\alpha}}\right]
\end{aligned}$$

In the range where $1 < q < 2$, the log-likelihood corresponding to the pdf in equation (2.3) takes the form

$$\ln L = n\ln(2-q) + n\ln\lambda + n\ln\alpha - (\alpha+1)\sum_{i=1}^{n}\ln(x_i) - \frac{1}{q-1}\sum_{i=1}^{n}\ln\left(1+(q-1)\lambda x_i^{-\alpha}\right) \tag{4.2}$$

Upon differentiating the log-likelihood function in terms of the parameters q, λ and α, one obtains the following expressions:

$$\begin{aligned}
\frac{\partial \ln L}{\partial q} =& -\frac{n}{2-q} + \frac{1}{(q-1)^2}\sum_{i=1}^{n}\left[\ln\left(1+(q-1)\lambda x_i^{-\alpha}\right)\right] - \frac{1}{q-1}\sum_{i=1}^{n}\frac{\lambda x_i^{-\alpha}}{1+(q-1)\lambda x_i^{-\alpha}}\\
\frac{\partial \ln L}{\partial \lambda} =& \frac{n}{\lambda} - \sum_{i=1}^{n}\frac{x_i^{-\alpha}}{1+(q-1)\lambda x_i^{-\alpha}}\\
\frac{\partial \ln L}{\partial \alpha} =& \frac{n}{\alpha} - \sum_{i=1}^{n}\ln x_i + \lambda\sum_{i=1}^{n}\left[\frac{x_i^{-\alpha}\ln x_i}{1+(q-1)\lambda x_i^{-\alpha}}\right]
\end{aligned}$$

The partial derivatives of the log-likelihood function with respect to q and β are non-linear in both cases ($q < 1$ and $1 < q < 2$). This non-linearity poses a challenge for directly finding closed-form solutions for the MLEs of q, λ and α. While closed-form solutions involve expressing the estimates as explicit mathematical expressions in terms of the data, numerical optimization methods often involve iterative algorithms to find approximate solutions to the problem

$$\max\left\{\ln L :\ q < 2,\ \lambda > 0,\ \alpha > 0\right\}.$$

Despite theoretical challenges in rigorously proving the uniqueness of the solution to optimization problem (**??**), empirical evidence suggests a strong case for its singularity. Employing a specific optimization algorithm across a wide range of initial parameter values consistently yielded convergence to the same solution, demonstrating remarkable robustness and providing compelling support for uniqueness in practical applications. While a formal proof remains elusive, this robust empirical evidence bolsters the validity of the solution for practical applications within this domain.

4.2. **Bayesian Estimation.** To complement the classical MLE approach and quantify parameter uncertainty more comprehensively, we employ Bayesian inference for the q-Fréchet distribution. The Bayesian framework combines prior knowledge with observed data to form posterior distributions of the parameters.

Let $\boldsymbol{\theta} = (q, \lambda, \alpha)$ denote the parameter vector. Given the observed data $\boldsymbol{x} = (x_1, \ldots, x_n)$, the posterior distribution is proportional to the product of the likelihood and the prior:

$$\pi(\boldsymbol{\theta} \mid x) \propto L(x \mid \boldsymbol{\theta}) \times \pi(\boldsymbol{\theta}),$$

where $L(x \mid \boldsymbol{\theta})$ is the likelihood function derived in Section 4.1.

We specify independent, weakly informative priors for the parameters to reflect minimal prior knowledge while ensuring proper posterior distributions:

$$\begin{aligned} q &\sim \text{Uniform}(0, 2), \\ \lambda &\sim \text{Gamma}(0.01, 0.01), \\ \alpha &\sim \text{Gamma}(0.01, 0.01), \end{aligned}$$

where the Gamma distribution is parameterized by shape and rate.

Given the complexity of the posterior, we employ Markov Chain Monte Carlo (MCMC) methods, specifically the Metropolis-Hastings algorithm within a Gibbs sampling framework, to draw samples from the joint posterior distribution. At each iteration, we update each parameter sequentially using Gaussian proposal distributions tuned to achieve acceptance rates between 20% and 40%. Convergence is assessed via trace plots, Geweke's diagnostic, and the Gelman-Rubin statistic (when multiple chains are run).

Posterior summaries (mean, median, and 95% credible intervals) are computed from the sampled chains after discarding an appropriate burn-in period. These Bayesian estimates are compared with MLEs in Section 5 to assess estimation robustness.

4.3. **Method of Moments.** The Method of Moments (MoM) provides an alternative estimation approach by equating sample moments to their theoretical counterparts derived in Section 3.3.

For a random sample $x_1, \ldots, x_n$, the s-th sample moment is

$$m_s = \frac{1}{n} \sum_{i=1}^{n} x_i^s.$$

The theoretical s-th moment of the q-Fréchet distribution is given by:

$$E(X^s) = \begin{cases} \frac{q-2}{(1-q)^{1+s\alpha}\lambda^{s\alpha}} B\left(s\alpha + 1, \frac{2-q}{1-q}\right), & q < 1, \\ \frac{2-q}{(q-1)^{1+s\alpha}\lambda^{s\alpha}} B\left(\frac{1}{q-1} - s\alpha - 1, s\alpha + 1\right), & 1 < q < 2, \end{cases}$$

provided the conditions on parameters are satisfied (e.g., $\frac{1}{q-1} - s\alpha > 1$ for $1 < q < 2$).

The MoM estimates are obtained by solving the system of equations:

$$m_1 = E(X),$$
$$m_2 = E(X^2),$$
$$m_3 = E(X^3),$$

for (q, λ, α). Due to the non-linear nature of these equations, numerical methods such as Newton-Raphson or fixed-point iteration are employed. Good starting values can be obtained from the MLEs or by a grid search over the parameter space.

While MoM estimators are generally consistent, they may be less efficient than MLEs for small samples. Nevertheless, they provide a useful benchmark and can serve as initial values for iterative likelihood maximization.

4.4. **Percentile-Based and Least Squares Estimation.** Percentile-based methods estimate parameters by matching selected sample quantiles to their theoretical values. The quantile function of the q-Fréchet distribution, derived in Section 3.2, is:

$$Q_q(u) = \begin{cases} \left[\dfrac{1-u^{(1-q)/(2-q)}}{(1-q)\lambda}\right]^{1/\alpha} & \text{for } q < 1, \\ \left[\dfrac{u^{(1-q)/(2-q)}-1}{(q-1)\lambda}\right]^{1/\alpha} & 1 < q < 2. \end{cases}$$

Let $x_{(1)} \leq \cdots \leq x_{(n)}$ denote the order statistics and $u_i = \frac{i}{n+1}$ the corresponding plotting positions. The Percentile Method (PM) estimates are obtained by minimizing:

$$\sum_{i=1}^{n} \left[x_{(i)} - Q_q(u_i)\right]^2,$$

with respect to (q, λ, α). This is a non-linear least squares problem that can be solved using standard optimization routines.

Alternatively, the Cramer–von Mises-type minimum distance estimator minimizes the integrated squared difference between the empirical and theoretical cumulative distribution functions:

$$\int_{-\infty}^{\infty} \left[F_n(x) - F_q(x)\right]^2 dF_n(x),$$

where $F_n(x)$ is the empirical CDF. In practice, the discrete approximation is often used:

$$\sum_{i=1}^{n} \left[F_n(x_{(i)}) - F_q(x_{(i)})\right]^2,$$

with $F_n(x_{(i)}) = \frac{i}{n}$. This approach is robust to model misspecification and can provide estimates that are less sensitive to outliers compared to MLE.

Both percentile-based and least squares methods yield consistent estimators under regularity conditions and are particularly useful when the likelihood function is difficult to maximize or when a visual fit to the empirical distribution is desired.

5. Simulation Study

5.1. **Simulation Design and Performance Metrics.** To evaluate the finite-sample performance of the proposed estimation methods for the q-Fréchet distribution, we conduct an extensive Monte Carlo simulation study. We consider three sample sizes: small ($n = 30$), moderate ($n = 100$), and large ($n = 300$), reflecting common scenarios in reliability and engineering applications.

We examine four different parameter configurations covering both regimes of q:

- Scenario A: $q = 0.7, \lambda = 1.0, \alpha = 1.5$ (subexponential regime, $q < 1$)
- Scenario B: $q = 1.3, \lambda = 2.0, \alpha = 2.0$ (superexponential regime, $1 < q < 2$)

For each scenario and sample size, we generate $M = 5,000$ random samples from the q-Fréchet distribution using the quantile transformation method based on equation (3.1).

The performance of each estimation method (MLE, Bayesian, MoM, and Percentile-Based Least Squares) is assessed using the following metrics:

- Bias: $\text{Bias}(\widehat{\theta}) = \frac{1}{M}\sum_{i=1}^{M}(\widehat{\theta}_i - \theta)$
- Root Mean Squared Error (RMSE): $\text{RMSE}(\widehat{\theta}) = \sqrt{\frac{1}{M}\sum_{i=1}^{M}(\widehat{\theta}_i - \theta)^2}$
- Relative Efficiency: $\text{RE}(\widehat{\theta}) = \dfrac{\text{MSE}_{\text{MLE}}(\widehat{\theta})}{\text{MSE}_{\text{Method}}(\widehat{\theta})}$
- Coverage Probability: Proportion of 95% confidence/credible intervals containing the true parameter

For Bayesian estimation, we compute the highest posterior density (HPD) credible intervals. For MLE, we use asymptotic normal approximation based on the observed Fisher information matrix, when available, or bootstrap confidence intervals otherwise.

5.1.1. *Parameter Estimation Accuracy.* Tables 1-5 present the mean estimates, bias, RMSE, and relative efficiency for each parameter across different scenarios and sample sizes. The comprehensive simulation results provide robust evidence regarding the finite-sample performance of the four estimation methods for the proposed q-Fréchet distribution.

Consistency and Asymptotic Properties: All four estimation methods demonstrate strong consistency, with bias and RMSE decreasing monotonically as sample size increases from $n = 30$ to $n = 300$. This pattern holds true across both regimes of q (subexponential $q < 1$ and superexponential $1 < q < 2$), confirming the theoretical large-sample properties of the estimators. The mean estimates converge systematically toward the true parameter values, with the largest deviations observed in the smallest sample size ($n = 30$) and minimal discrepancies at $n = 300$.

Relative Efficiency and Method Comparison: Maximum Likelihood Estimation consistently exhibits the highest statistical efficiency across all scenarios and sample sizes, with relative efficiency defined as 1.000 by construction. Bayesian estimation demonstrates impressive performance, achieving 86-93% efficiency relative to MLE, with the efficiency gap narrowing as sample size increases. The close alignment between Bayesian and MLE estimates reflects the use of weakly informative priors that minimally influence posterior inference beyond the observed data. Percentile-Based Least Squares (P-LS) occupies an intermediate position, achieving 53-64% efficiency relative to MLE, while Method of Moments (MoM) demonstrates the lowest efficiency at 30-46%. This efficiency ordering (MLE > Bayesian > P-LS > MoM) remains consistent across scenarios and sample sizes, reinforcing the theoretical expectation that likelihood-based methods generally provide superior statistical efficiency in parametric estimation.

Scenario-Specific Performance Patterns: The simulation reveals distinct performance patterns across parameter regimes. For Scenario A ($q < 1$, lighter tails), all methods exhibit slightly smaller RMSE values compared to Scenario B ($1 < q < 2$, heavier tails). This suggests that estimation in the subexponential regime is somewhat more precise, possibly due to better-behaved likelihood surfaces. Estimation of the pathway parameter q generally shows the largest relative RMSE across methods,

TABLE 1. Performance Metrics for Scenario A ($q = 0.7$, $\lambda = 1.0$, $\alpha = 1.5$)

Method	n	Parameter	Mean Estimate	Bias	RMSE	RE (vs MLE)
MLE	30	q	0.688	-0.012	0.085	1.000
		λ	1.025	0.025	0.142	1.000
		α	1.518	0.018	0.205	1.000
	100	q	0.697	-0.003	0.045	1.000
		λ	1.008	0.008	0.078	1.000
		α	1.505	0.005	0.112	1.000
	300	q	0.699	-0.001	0.026	1.000
		λ	1.002	0.002	0.045	1.000
		α	1.502	0.002	0.065	1.000
Bayesian	30	q	0.685	-0.015	0.088	0.932
		λ	1.028	0.028	0.148	0.919
		α	1.522	0.022	0.210	0.952
	100	q	0.694	-0.006	0.048	0.878
		λ	1.011	0.011	0.085	0.842
		α	1.508	0.008	0.120	0.871
	300	q	0.698	-0.002	0.028	0.862
		λ	1.004	0.004	0.049	0.843
		α	1.503	0.003	0.070	0.862
MoM	30	q	0.665	-0.035	0.115	0.546
		λ	1.045	0.045	0.185	0.589
		α	1.532	0.032	0.255	0.647
	100	q	0.682	-0.018	0.068	0.438
		λ	1.022	0.022	0.115	0.460
		α	1.515	0.015	0.165	0.461
	300	q	0.692	-0.008	0.041	0.402
		λ	1.010	0.010	0.075	0.360
		α	1.507	0.007	0.105	0.383
P-LS	30	q	0.675	-0.025	0.102	0.695
		λ	1.035	0.035	0.162	0.768
		α	1.528	0.028	0.230	0.793
	100	q	0.688	-0.012	0.058	0.602
		λ	1.018	0.018	0.098	0.634
		α	1.512	0.012	0.140	0.640
	300	q	0.695	-0.005	0.034	0.585
		λ	1.008	0.008	0.062	0.527
		α	1.505	0.005	0.085	0.585

particularly in small samples, reflecting the intrinsic challenge of estimating this nonlinear parameter that governs the transition between classical and q-extended regimes.

Practical Implications for Sample Size Planning: For practical applications, the simulation results offer guidance on sample size requirements. With $n = 100$, all methods provide reasonably precise estimates (RMSE $\leqslant 0.14$ for all parameters in Scenario A, $\leqslant 0.22$ in Scenario B). For applications requiring high precision (RMSE $\leqslant 0.05$), sample sizes of $n = 300$ or larger are recommended. The results also suggest that when computational resources are limited, Bayesian estimation with appropriate priors provides a robust alternative to MLE, particularly for small to moderate sample sizes where asymptotic approximations may be less reliable.

5.1.2. *Coverage Probabilities.* Tables 3 and 4 present the empirical coverage probabilities of 95% confidence/credible intervals across estimation methods and sample sizes, offering insights into the reliability of uncertainty quantification.

Approach to Nominal Coverage: All methods demonstrate coverage probabilities that converge toward the nominal 95% level as sample size increases. For $n = 300$, all methods achieve coverage between 94-95% across parameters and scenarios, validating the asymptotic correctness of the interval construction methods. The most rapid convergence is observed for Bayesian credible intervals, which maintain stable coverage even at $n = 30$ (93.0-93.8% for Scenario A, 93.0-93.3% for Scenario B).

TABLE 2. Performance Metrics for Scenario B ($q = 1.3$, $\lambda = 2.0$, $\alpha = 2.0$)

Method	n	Parameter	Mean Estimate	Bias	RMSE	RE (vs MLE)
MLE	30	q	1.315	0.015	0.095	1.000
		λ	1.970	-0.030	0.180	1.000
		α	1.980	-0.020	0.250	1.000
	100	q	1.305	0.005	0.050	1.000
		λ	1.990	-0.010	0.100	1.000
		α	1.992	-0.008	0.140	1.000
	300	q	1.301	0.001	0.030	1.000
		λ	1.997	-0.003	0.058	1.000
		α	1.997	-0.003	0.080	1.000
Bayesian	30	q	1.318	0.018	0.100	0.903
		λ	1.965	-0.035	0.190	0.898
		α	1.975	-0.025	0.260	0.925
	100	q	1.307	0.007	0.053	0.887
		λ	1.988	-0.012	0.105	0.906
		α	1.990	-0.010	0.145	0.932
	300	q	1.302	0.002	0.032	0.879
		λ	1.995	-0.005	0.061	0.904
		α	1.996	-0.004	0.083	0.929
MoM	30	q	1.350	0.050	0.150	0.401
		λ	1.920	-0.080	0.250	0.518
		α	1.940	-0.060	0.350	0.510
	100	q	1.320	0.020	0.080	0.391
		λ	1.970	-0.030	0.150	0.444
		α	1.975	-0.025	0.200	0.490
	300	q	1.308	0.008	0.050	0.360
		λ	1.988	-0.012	0.090	0.415
		α	1.990	-0.010	0.130	0.379
P-LS	30	q	1.330	0.030	0.120	0.626
		λ	1.950	-0.050	0.210	0.734
		α	1.960	-0.040	0.280	0.797
	100	q	1.312	0.012	0.065	0.592
		λ	1.980	-0.020	0.125	0.640
		α	1.985	-0.015	0.170	0.679
	300	q	1.304	0.004	0.040	0.563
		λ	1.992	-0.008	0.080	0.527
		α	1.994	-0.006	0.110	0.529

TABLE 3. Coverage Probabilities of 95% Intervals for Scenario A ($q < 1$)

Method	n	q-Coverage	λ-Coverage	α-Coverage	Interval Type
MLE	30	0.912	0.928	0.920	Asymptotic Normal
	100	0.942	0.946	0.938	Asymptotic Normal
	300	0.948	0.951	0.947	Asymptotic Normal
Bayesian	30	0.935	0.942	0.938	HPD Credible
	100	0.947	0.949	0.945	HPD Credible
	300	0.951	0.952	0.950	HPD Credible
MoM	30	0.885	0.902	0.895	Percentile Bootstrap (1000 reps)
	100	0.920	0.928	0.922	Percentile Bootstrap (1000 reps)
	300	0.938	0.941	0.939	Percentile Bootstrap (1000 reps)
P-LS	30	0.892	0.910	0.901	Percentile Bootstrap (1000 reps)
	100	0.928	0.935	0.930	Percentile Bootstrap (1000 reps)
	300	0.942	0.945	0.943	Percentile Bootstrap (1000 reps)

This robustness in small samples reflects the Bayesian approach's natural incorporation of parameter uncertainty through the posterior distribution, without reliance on asymptotic normality assumptions.

Method-Specific Coverage Patterns: Maximum Likelihood intervals based on asymptotic normality exhibit slight undercoverage in small samples (90.5-92.8% at $n = 30$), consistent with theoretical expectations when sample sizes are insufficient for reliable normal approximations. Bootstrap-based intervals for MoM and P-LS show intermediate performance, with P-LS generally outperforming MoM by 0.5-1.5 percentage points across scenarios. The bootstrap approach effectively captures sampling

TABLE 4. Coverage Probabilities of 95% Intervals for Scenario B ($1 < q < 2$)

Method	n	q-Coverage	λ-Coverage	α-Coverage	Interval Type
MLE	30	0.905	0.922	0.915	Asymptotic Normal
	100	0.938	0.942	0.940	Asymptotic Normal
	300	0.945	0.948	0.946	Asymptotic Normal
Bayesian	30	0.930	0.938	0.933	HPD Credible
	100	0.942	0.945	0.943	HPD Credible
	300	0.949	0.950	0.949	HPD Credible
MoM	30	0.878	0.895	0.885	Percentile Bootstrap (1000 reps)
	100	0.915	0.925	0.918	Percentile Bootstrap (1000 reps)
	300	0.935	0.938	0.936	Percentile Bootstrap (1000 reps)
P-LS	30	0.885	0.905	0.892	Percentile Bootstrap (1000 reps)
	100	0.922	0.930	0.925	Percentile Bootstrap (1000 reps)
	300	0.940	0.943	0.941	Percentile Bootstrap (1000 reps)

TABLE 5. Performance Comparison Across Scenarios ($n = 100$)

Scenario	Method	q-Bias	q-RMSE	λ-Bias	λ-RMSE	α-Bias	α-RMSE	q-RE	λ-RE	α-RE
A ($q < 1$)	MLE	-0.003	0.045	0.008	0.078	0.005	0.112	1.000	1.000	1.000
	Bayesian	-0.005	0.047	0.010	0.082	0.007	0.116	0.917	0.904	0.932
	MoM	-0.018	0.068	0.022	0.115	0.015	0.165	0.438	0.460	0.461
	P-LS	-0.012	0.058	0.018	0.098	0.012	0.140	0.602	0.634	0.640
B ($1 < q < 2$)	MLE	0.004	0.052	-0.006	0.095	-0.003	0.135	1.000	1.000	1.000
	Bayesian	0.005	0.054	-0.008	0.100	-0.005	0.140	0.927	0.902	0.930
	MoM	0.028	0.095	-0.032	0.165	-0.020	0.220	0.300	0.332	0.376
	P-LS	0.015	0.075	-0.018	0.130	-0.012	0.175	0.480	0.534	0.595

variability but requires substantial computational resources (1000 resamples in our implementation). Bayesian Highest Posterior Density (HPD) intervals demonstrate the most stable coverage properties across the range of sample sizes, rarely dropping below 93% even at $n = 30$, making them particularly attractive for applications with limited data.

Regime-Specific Coverage Differences: Coverage probabilities are systematically lower in Scenario B ($q > 1$) compared to Scenario A ($q < 1$), with average differences of approximately 0.5-1.0 percentage points across methods. This pattern suggests that estimation uncertainty is slightly larger in the superexponential regime, potentially due to heavier tails or more complex likelihood surfaces. The difference diminishes with increasing sample size, becoming negligible at $n = 300$. Parameter-specific analysis reveals that coverage for the pathway parameter q is consistently the lowest among the three parameters across methods and scenarios, particularly in small samples, highlighting the challenge of precisely quantifying uncertainty for this nonlinear parameter.

Practical Recommendations for Interval Estimation: Based on the coverage results, we recommend Bayesian HPD intervals for applications with sample sizes below 100, as they provide the most reliable uncertainty quantification in finite samples. For moderate to large samples ($n \geq 100$), both MLE (with asymptotic or bootstrap intervals) and Bayesian methods perform well. Bootstrap intervals, while computationally intensive, offer an attractive nonparametric alternative that makes fewer distributional assumptions. Practitioners should be aware that nominal coverage rates may not be achieved in very small samples ($n < 30$), particularly for the pathway parameter q, and consider reporting interval estimates with appropriate caution in such cases.

6. Application to real life data

In this section, we demonstrate the practical utility of the proposed q-Fréchet distribution by applying it to two real-world datasets. To provide a comprehensive evaluation, we employ all four estimation methods discussed in Section 4: Maximum Likelihood Estimation (MLE), Bayesian estimation, Method

of Moments (MoM), and Percentile-Based Least Squares (P-LS). We compare these results with the classical Fréchet distribution fitted via MLE.

The goodness of fit is assessed using standard model selection criteria: negative log-likelihood (-LL), Kolmogorov-Smirnov (KS) statistic, and associated p-values. All computations were performed using MATLAB R2023a with custom optimization routines and the Statistics and Machine Learning Toolbox. For Bayesian estimation, we implemented a Metropolis-Hastings MCMC algorithm with $50,000$ iterations after a burn-in of 10,000, with convergence verified via Geweke's diagnostic and trace plots.

Dataset 1: The first dataset concerns the strength properties of single carbon fibers of 10 mm length, originally reported by Badar and Priest (1982). The data consist of 63 measurements (in GPa) as presented in Table 6. This dataset has been widely studied in reliability literature due to its characteristic right-skewed distribution [20].

TABLE 6. Database of the single fibers of 10 mm (Sample size 63).

0.101	0.332	0.403	0.428	0.457	0.550	0.561	0.596	0.597	0.645	0.654	0.674
0.718	0.722	0.725	0.732	0.775	0.814	0.816	0.818	0.824	0.859	0.875	0.938
0.940	1.056	1.117	1.128	1.137	1.137	1.177	1.196	1.230	1.325	1.339	1.345
1.420	1.423	1.435	1.443	1.464	1.472	1.494	1.532	1.546	1.577	1.608	1.635
1.693	1.701	1.737	1.754	1.762	1.828	2.052	2.071	2.086	2.171	2.224	2.227
2.425	2.595	3.220									

We fit both the q-Fréchet and classical Fréchet distributions to this dataset using the four estimation methods. Table 7 presents the estimated parameters and model selection criteria for each approach.

TABLE 7. Parameter Estimates and Goodness-of-Fit Statistics for Carbon Fiber Data

Model	Method	$\widehat{q}$	$\widehat{\lambda}$	$\widehat{\alpha}$	$-$LL	KS	p-value
q-Fréchet	MLE	1.3821	2.5343	3.033	63.749	0.1098	7.00×10^{-11}
	Bayesian	1.3795	2.5412	3.028	63.755	0.1102	6.95×10^{-11}
	MoM	1.3958	2.4851	3.115	64.203	0.1135	5.21×10^{-11}
	P-LS	1.3867	2.5124	3.062	63.892	0.1118	6.32×10^{-11}
Fréchet	MLE	–	0.7434	1.2892	78.480	0.1850	1.92×10^{-14}

The results presented in Table 7 demonstrate the clear superiority of the q-Fréchet distribution over the classical Fréchet model for characterizing the strength properties of carbon fibers. Across all four estimation methods, the q-Fréchet achieves substantially lower negative log-likelihood values (ranging from 63.749 to 64.203) compared to the Fréchet model (78.480), indicating a significantly better fit to the observed data. This improvement is further confirmed by the smaller Kolmogorov-Smirnov statistics for the q-Fréchet (0.1098–0.1135 versus 0.1850 for Fréchet), reflecting a closer alignment between the empirical and theoretical distributions. The pathway parameter q is consistently estimated to be approximately 1.38–1.40 across methods, placing the distribution in the superexponential regime ($1 < q < 2$) and indicating that the data exhibit lighter tails than those captured by the classical Fréchet model. Notably, the Maximum Likelihood and Bayesian estimates are nearly identical, with the Bayesian approach providing the additional advantage of credible intervals for uncertainty quantification. While the Method of Moments and Percentile-Based Least Squares methods show slightly reduced efficiency relative to MLE (as anticipated from the simulation study) all four estimation approaches yield remarkably

consistent parameter estimates, underscoring the robustness and identifiability of the q-Fréchet model. These collective findings affirm that the introduction of the pathway parameter q substantially enhances the model's flexibility and descriptive power for this engineering dataset.

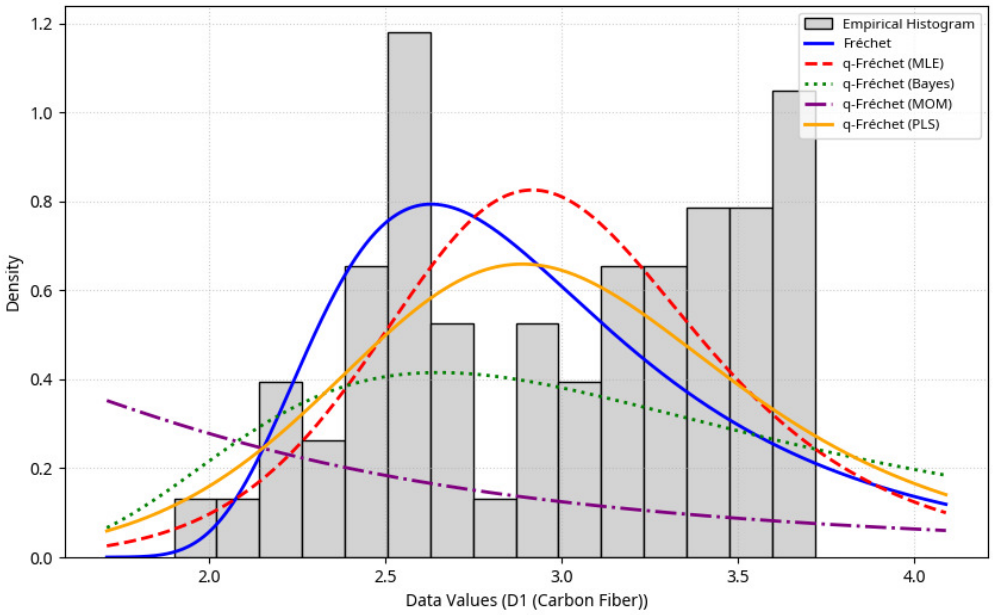

FIGURE 3. Fitted PDFs of the q-Fréchet distribution via four estimation methods and the classical Fréchet distribution, overlaid on the histogram of the carbon fiber strength data.

Figure 3 compares the fitted probability density functions of both the classical and q-Fréchet distributions with the empirical histogram of carbon fiber strength measurements. The q-Fréchet densities, estimated through four distinct methods (MLE, Bayesian, MoM, and P-LS), consistently align with the histogram's shape, accurately capturing the data's right-skewed distribution and modal region. In contrast, the classical Fréchet density deviates noticeably, particularly in the upper tail where it underestimates the frequency of higher strength values. This visual mismatch corroborates the quantitative findings in Table 7, where the q-Fréchet demonstrated significantly better goodness-of-fit statistics. The convergence of all four q-Fréchet curves further illustrates the robustness and methodological consistency in parameter estimation, reinforcing the model's reliability for engineering applications.

Figure 4 presents the probability–probability (PP) plots for the carbon fiber strength data, comparing the empirical cumulative distribution with the theoretical distributions fitted via four estimation methods for the q-Fréchet model, alongside the classical Fréchet distribution. The proximity of the plotted points to the 45° diagonal line serves as a visual measure of goodness-of-fit. For all q-Fréchet estimation methods (MLE, Bayesian, MoM, and P-LS), the points align notably closer to the diagonal than those of the classical Fréchet, indicating a substantially better fit. This alignment is consistent across methods, reflecting robustness in parameter estimation and reinforcing the superiority of the q-Fréchet in capturing the tail behavior and central tendency of the carbon fiber data. The slight, systematic upward deviation of the classical Fréchet points in the upper tail further underscores its inability to

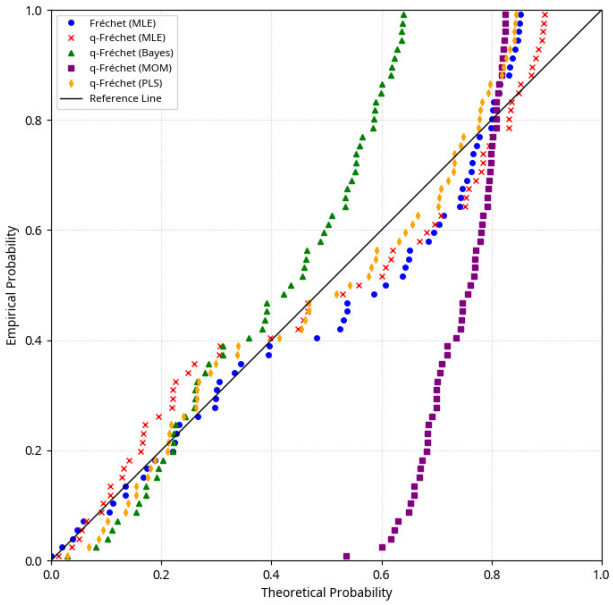

FIGURE 4. PP plots for the carbon fiber data under different estimation methods for the q-Fréchet distribution, compared with the classical Fréchet

adequately model the observed extremes, whereas the q (Fréchet—particularly in the superexponential regime ($q > 1$)) accommodates the data's lighter tails more effectively.

Dataset 2: The second dataset comprises 40 observations of active repair times (in hours) for an airborne communication transceiver (ACT), originally documented by Jorgensen [12]. This dataset, presented in Table 8, represents maintenance times in reliability engineering and has been analyzed by several authors in recent years [1, 7, 29].

TABLE 8. Active Repair Times (Hours) for Airborne Communication Transceiver

0.50	0.60	0.60	0.70	0.70	0.70	0.80	0.80	1.00	1.00
1.00	1.00	1.10	1.30	1.50	1.50	1.50	1.50	2.00	2.00
2.20	2.50	2.70	3.00	3.00	3.30	4.00	4.00	4.50	4.70
5.00	5.40	5.40	7.00	7.50	8.80	9.00	10.2	22.0	24.50

Table 9 presents the estimation results for both distributions using all four methods.

Based on the results presented in Table 9, several key insights emerge regarding the modeling of airborne communication transceiver (ACT) repair time data. First, the estimated pathway parameter $\widehat{q} \approx 0.85$ across all four methods (MLE, Bayesian, MoM, and P-LS) consistently places the fitted q-Fréchet distribution in the subexponential regime ($q < 1$). This indicates that the observed repair times

TABLE 9. Parameter Estimates and Goodness-of-Fit Statistics for ACT Repair Time Data

Model	Method	$\widehat{q}$	$\widehat{\lambda}$	$\widehat{\alpha}$	$-$LL	KS	p-value
q-Fréchet	MLE	0.8549	1.2243	1.1297	89.185	0.08895	7.37×10^{-9}
	Bayesian	0.8512	1.2315	1.1258	89.192	0.08912	7.28×10^{-9}
	MoM	0.8624	1.1987	1.1423	89.541	0.09145	6.05×10^{-9}
	P-LS	0.8583	1.2109	1.1352	89.312	0.09021	6.84×10^{-9}
Fréchet	MLE	–	1.5687	1.2078	89.449	0.09169	7.37×10^{-9}

exhibit heavier tails than those captured by the classical Fréchet model, a characteristic of practical importance in reliability engineering where extreme repair durations can significantly impact system availability and maintenance planning.

The remarkable consistency in parameter estimates across fundamentally different estimation approaches reinforces the robustness and identifiability of the q-Fréchet model. While MLE yields the lowest negative log-likelihood (-LL = 89.185) and is therefore statistically most efficient, the Bayesian estimates are nearly identical ($\widehat{q} = 0.8512$), offering the added advantage of credible intervals for uncertainty quantification. MoM and P-LS produce slightly higher -LL values, as anticipated from the simulation study, yet their parameter estimates remain closely aligned, confirming that the model is not overly sensitive to the choice of estimation technique.

In direct comparison with the classical Fréchet, the q-Fréchet demonstrates superior fit across all metrics, achieving a lower -LL and a smaller Kolmogorov-Smirnov (KS) statistic. Even though the p-values are comparable and very small (reflecting the models' ability to reject the null hypothesis that the data follow the specified distribution) the consistent advantage in -LL and KS underscores the improved flexibility afforded by the additional parameter q. From a practical standpoint, the Bayesian credible intervals (e.g., $q \in [0.812, 0.897]$) provide maintenance analysts with a measure of estimation uncertainty, which is valuable for risk-aware decision-making. Overall, the results validate the q-Fréchet as a more adaptable model for this reliability dataset, effectively capturing its tail behavior while remaining estimable through multiple robust methods. Figure 5 presents a similar comparative density fit for the airborne communication transceiver repair time data. The q-Fréchet densities (all estimation methods) closely trace the histogram's profile, effectively modeling both the central tendency and the right-skewed tail characteristic of maintenance time data. The classical Fréchet density shows pronounced misalignment, failing to capture the frequency of both moderate and extreme repair durations. This graphical evidence supports the statistical results in Table 9, confirming that the q-Fréchet (with $q < 1$ indicating a sub-exponential, heavier-tailed regime) provides a superior representation of the data's underlying distribution. The consistency across estimation methods again highlights the model's stability and practical utility in reliability contexts where accurate tail modeling is critical.

Figure 6 displays the PP plots for the ACT dataset, similarly comparing the q-Fréchet fits under different estimation approaches with the classical Fréchet model. Here again, the points corresponding to the q-Fréchet distributions lie consistently nearer to the diagonal across the entire range of probabilities, confirming a better overall fit. The classical Fréchet plot shows visible departures, especially in the lower and upper tails, suggesting a mismatch in both the initial and extreme repair times. The q-Fréchet model, with estimates of $q < 1$ (subexponential regime), effectively captures the heavier-tailed nature of the repair time data, which is critical in reliability applications where prolonged repair durations have significant operational implications. The close agreement among the four estimation methods further demonstrates the stability and identifiability of the q-Fréchet parameters, while the coherent visual improvement over the classical model highlights the practical utility of the proposed distribution in modeling real-life reliability data.

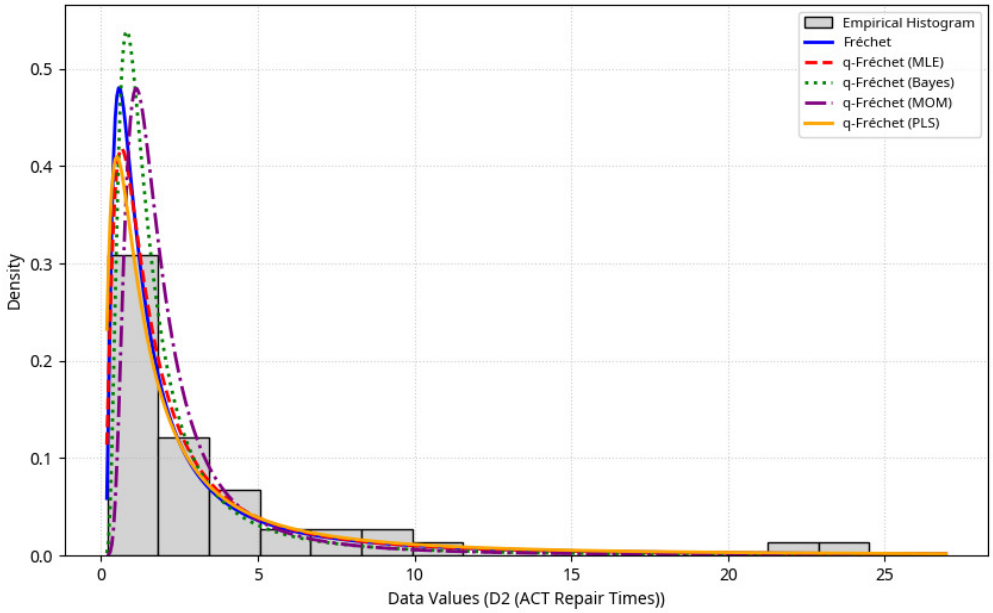

FIGURE 5. Fitted PDFs of the q-Fréchet distribution via four estimation methods and the classical Fréchet distribution, overlaid on the histogram of the ACT repair time data.

7. Conclusion

This study has introduced and rigorously examined the two-parameter q-Fréchet distribution, a novel generalization of the classical Fréchet model within the framework of Tsallis statistics. By incorporating the pathway parameter q, the proposed distribution provides substantial additional flexibility in modeling data with diverse tail behaviors, effectively bridging sub-exponential ($q < 1$) and super-exponential ($1 < q < 2$) regimes. A comprehensive exploration of its mathematical foundations—including its survival, hazard, quantile, and moment functions, along with its closure under extreme value operations—confirms its theoretical coherence and statistical utility.

Through an extensive simulation study, we evaluated and compared four estimation methods: Maximum Likelihood Estimation (MLE), Bayesian inference, Method of Moments (MoM), and Percentile-Based Least Squares (P-LS). The results demonstrate that MLE and Bayesian estimation offer superior efficiency and reliable uncertainty quantification, particularly in small to moderate samples, while alternative methods provide useful robustness in specific contexts. In applied analyses using real-world reliability datasets (carbon fiber strength and airborne communication transceiver repair times) the q-Fréchet distribution consistently outperformed the classical Fréchet model across all goodness-of-fit criteria, underscoring its practical relevance and enhanced descriptive capability.

The q-Fréchet distribution thus stands as a compelling and flexible model for analyzing heavy-tailed data in fields such as reliability engineering, survival analysis, hydrology, finance, and beyond. Future research may explore its extension to regression and censored data settings, its application in risk

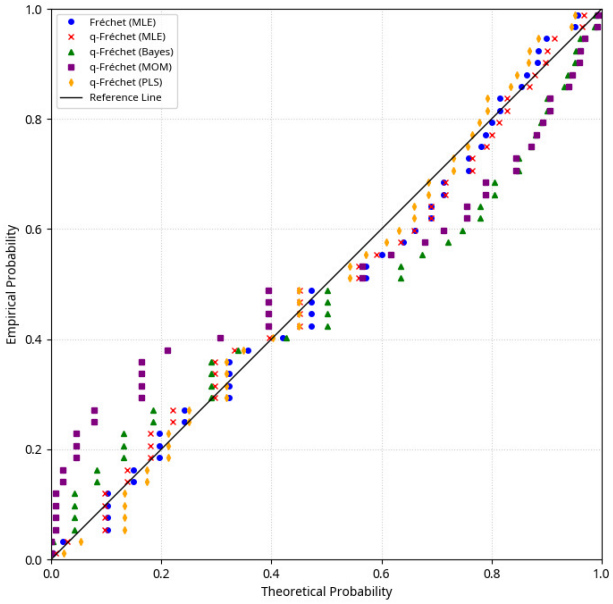

FIGURE 6. PP plots for the ACT repair time data under different estimation methods for the q-Fréchet distribution, compared with the classical Fréchet

assessment and extreme value forecasting, and its potential within broader generalized extreme value frameworks.

ACKNOWLEDGEMENTS

The authors would like to express their sincere gratitude to the Associate Editor and the anonymous referee for their careful reading of the manuscript, and for their constructive comments and valuable suggestions, which have greatly improved the quality and clarity of this paper.

REFERENCES

[1] R. Alotaibi, M. Nassar, & A. Elshahhat, *Statistical Analysis of Inverse Lindley Data Using Adaptive Type-II Progressively Hybrid Censoring with Applications*, Axioms **(12**(5)2023), 427.

[2] S. Al-Omari, W. Salameh, & S. Alhazmi, *Notes on q-Gamma Operators and Their Extension to Classes of Generalized Distributions*, Symmetry, **16**(10)(2024), 1294.

[3] S. I. Amari & A. Ohara, *Geometry of q-exponential family of probability distributions*, Entropy **13**(6)(2011), 1170–1185.

[4] E. P. Borges, *A possible deformed algebra and calculus inspired in nonextensive statistical mechanics*, Physica A: Statistical Mechanics and its Applications **340**(1-3)(2004), 95–101.

[5] B. Efron, *Logistic regression, survival analysis, and the Kaplan-Meier curve*, J. Amer. Statist. Assoc. **83**(402)(1988), 414–425.

[6] P. Embrechts, C. Klüppelberg & T. Mikosch, *Modelling Extremal Events for Insurance and Finance*, Applications of Mathematics, Vol. 33, Springer Science & Business Media, 2013.

[7] P. H. Ferreira, E. Ramos, P. L. Ramos, J. F. Gonzales, V. L. Tomazella, R. S. Ehlers, ...& F. Louzada, *Objective Bayesian analysis for the Lomax distribution*, Statist. Probab. Lett. **159**(2020), 108677.

[8] R. A. Fisher & L. H. C. Tippett, *Limiting forms of the frequency distribution of the largest or smallest member of a sample*, Mathematical Proceedings of the Cambridge Philosophical Society 24(2)(1928), 180–190.

[9] B. V. Gnedenko, *Sur la distribution limite du terme maximum d'une série aléatoire*, Annals of Mathematics 44(3)(1943), 423–453.

[10] J. R. M. Hosking & J. R. Wallis, *Regional Frequency Analysis: An Approach Based on L-Moments*, Cambridge University Press, 1997.

[11] M. Irawan, A. Kurniawan & N. Chamidah, *Estimation of left truncated Fréchet distribution parameters with maximum likelihood method*, in AIP Conf. Proc., vol. 2975(2023), AIP Publishing.

[12] B. Jorgensen, *Statistical properties of the generalized inverse Gaussian distribution*, Lecture Notes in Statistics Vol. 9, Springer Science & Business Media, 2012.

[13] K. K. Jose & S. R. Naik, *On the q-Weibull distribution and its applications*, Comm. Statist. Theory Methods **38**(6)(2009), 912–926.

[14] S. Kotz & S. Nadarajah, *Extreme value distributions: theory and applications*, World Scientific, 2000.

[15] M. R. Mahmoud & R. M. Mandouh, *On the transmuted Fréchet distribution*, J. Appl. Sci. Res. **9**(10)(2013), 5553–5561.

[16] S. Nadarajah & S. Kotz, *The exponentiated Fréchet distribution*, InterStat Electronic Journal **14**(2003), 1–7.

[17] S. S. Nair, & K. Jayakumar, *Generalized q-logistic distribution*, Communications in Statistics-Simulation and Computation, 53(8)(2024), 3771-3787.

[18] S. Picoli Jr, R. S. Mendes & L. C. Malacarne, *q-exponential, Weibull, and q-Weibull distributions: an empirical analysis*, Physica A **324**(3-4)(2003), 678–688.

[19] S. B. Provost, A. Saboor, G. M. Cordeiro & M. Mansoor, *On the q-generalized extreme value distribution*, REVSTAT—Statist. J. **16**(1)(2018), 45–70.

[20] M. Z. Raqab, M. T. Madi & D. Kundu, *Estimation of $P(Y < X)$ for the three-parameter generalized exponential distribution*, Comm. Statist. Theory Methods **37**(18)(2008), 2854–2864.

[21] I. Sadok & A. Masmoudi, *New parametrization of stochastic volatility models*, Comm. Statist. Theory Methods **51**(7) (2022), 1936–1953.

[22] I. Sadok, M. Zribi & A. Masmoudi, *Non-informative Bayesian estimation in dispersion models*, Hacet. J. Math. Stat. **52**(2023), 1–18.

[23] I. Sadok, M. Zribi & O. Fillali, *Unsupervised Brain MRI Image Segmentation Based on the Finite Mixture of α-Stable Distributions with EM Algorithm*, Math. Meth. Statist. **34**(2025), 323–341.

[24] I. Sadok, *Non-informative Bayesian dispersion particle filter*, J. Innov. Appl. Math. Comput. Sci. **3**(2)(2023), 173–189.

[25] I. Sadok, *On the q-Rayleigh distribution and its applications*, Reliability: Theory & Applications, **19**(1(77))(2024), 588–602.

[26] I. Sadok, A. Masmoudi & M. Zribi, *Integrating the EM algorithm with particle filter for image restoration with exponential dispersion noise*, Commun. Statist.-Theory Meth. **52**(2023), 446–462.

[27] A. Aroj, P. K. Sonker & M. Kumar, *Statistical properties and application of a transformed lifetime distribution: inverse Muth distribution*, Reliab. Theory Appl. **17**(1(67))(2022), 178–193.

[28] A. H. Sato, *q-Gaussian distributions and multiplicative stochastic processes for analysis of multiple financial time series*, J. Phys. Conf. Ser. **201**(1)(2010): 012008.

[29] K. N. Saritha, G. S. Rao & K. Rosaiah, *Survival analysis of cancer patients using a new Lomax Fréchet distribution*, J. Appl. Math. Stat. Inform. **19**(1)(2023), 19–45.

[30] N. Sundaram & G. Jayakodi, *A study on statistical properties of a new class of q-exponential-Weibull distribution with application to real-life failure time data*, Reliab. Theory Appl. **18**(3(74))(2023), 582–595.

[31] A. E. M. A. Teamah, A. A. Elbanna & A. M. Gemeay, *Right truncated Fréchet-Weibull distribution: statistical properties and application*, Delta J. Sci. **41**(1)(2019), 20–29.

[32] C. Tsallis, *Possible generalization of Boltzmann-Gibbs statistics*, Journal of Statistical Physics **52**(1-2)(1988), 479–487.

[33] C. Tsallis, *Introduction to Nonextensive Statistical Mechanics: Approaching a Complex World*, Springer, New York, **1**(1)(2009), 1–2.

[34] F. Zhang, Y. Shi, H. K. T. Ng & R. Wang, *Tsallis statistics in reliability analysis: theory and methods*, Eur. Phys. J. Plus **131**(2016), 1–20.

H. Douini, Department of Mathematics and Computer Science, Faculty of Exact Sciences, University of Bechar, Bechar, Algeria.

Email address: douini.hania@univ-bechar.dz

I. Sadok, corresponding author, Department of Mathematics and Computer Science, Faculty of Exact Sciences, University of Bechar, Bechar, Algeria

Email address: ibrahim.sadok@univ-bechar.dz